Signatures of chaotic tunneling

Amaury Mouchet*
Laboratoire de Mathématiques et de Physique Théorique, Université François Rabelais, Avenue Monge, Parc de Grandmont 37200 Tours, France†

Dominique Delande‡
Laboratoire Kastler-Brossel, Université Pierre et Marie Curie, 4, place Jussieu, F-75005 Paris, France
(Received 11 December 2002; published 25 April 2003)

Recent experiments with cold atoms provide a significant step toward a better understanding of tunneling when irregular dynamics is present at the classical level. In this paper, we lay out numerical studies that shed light on the previous experiments and help to clarify the underlying physics. This study also provides guidelines for future experiments.

DOI: 10.1103/PhysRevE.67.046216 PACS number(s): 05.45.Mt, 05.60.Gg, 32.80.Qk, 05.45.Pq

I. INTRODUCTION

When studying tunneling in nonseparable systems with more than one degree of freedom, one immediately encounters difficulties which generally can be traced back to the absence of sufficient constants of motion. Even in the very particular case of integrable systems, where continuous symmetries provide as many constants of motion as degrees of freedom, as soon as separability is lost, the analysis of tunneling is not a simple generalization of what occurs in one-dimensional (1D) autonomous systems. The latter case is detailed in textbooks on quantum physics (see, for instance, Ref. [1]) and it has even been possible to give a comprehensive analytical treatment in term of complex solutions of the Hamilton equations [2]. However, it was not until the mid-1980's that a satisfactory quantitative approach was proposed [3,4] for tunneling in nonseparable integrable systems involving a larger number of dimensions. Moreover, integrability is a property of higher-dimensional systems which is not generic. The coupling between several internal degrees of freedom as well as the coupling to an external source usually destroys some global constants of motion. With such a lack of constraints on the dynamics, the classical motion in phase space may become chaotic: it may explore volumes with higher dimensionality and therefore becomes exponentially sensitive to the initial conditions. It is not surprising that these deep qualitative differences between an integrable regime and a chaotic one appear at the quantum level, too. Some of the properties of a *quantum* system do change when constants of motion are broken. Indeed, it is the very object of quantum chaos to study the signatures of classical chaos at the quantum level (see for instance, Ref. [5] to realize how rich, vivid, and successful this domain is).

We define tunneling as a quantum process which is forbidden in *real* classical solutions of classical equations of motion. In this paper, we consider Hamiltonian systems only and study how the nondissipative breakdown of continuous symmetries affects tunneling. We do not consider how tunneling is modified by dissipation and decoherence of the quantum wave. Of course, this requires great care in real experiments, where making dissipation negligible is always a hard task. This is one of the main reasons why very few real experiments have been done on these questions. Such experiments would definitely help to understand tunneling in the presence of chaos (as far as we know, the only experiments explicitly made on chaotic tunneling in the 20th century are those presented in Ref. [6] with electromagnetic microwaves instead of quantum waves).

During the past 15 years, however, theoretical and numerical investigations on autonomous 2D and time-dependent 1D Hamiltonian systems have highlighted some mechanisms [3,4,7–12] and substantial information has been collected on the influence of nonseparable dynamics. Experimental evidence of such mechanisms would be of great interest, especially in light of the subtle interplay between interferences and disorder. These phenomena lie in the general context of wave transport in complex media where the role of disorder is played by the (deterministic) chaotic dynamics instead of having a statistical random origin. Of course, other important motivations can be found in the numerous domains where tunneling plays a crucial role as a fundamental quantum process: ionization [13], absorption, nuclear radioactivity, molecular collisions, mesoscopic physics etc. More speculatively, studies on tunneling in high-dimensional Hamiltonian systems should provide us with a natural extension of the instanton techniques. These techniques deal with quantum field theories which are reducible to effective 1D autonomous Lagrangian systems.

In 2001, it was shown both theoretically [14] and experimentally [15–18] that atom cooling techniques [19] (and possibly molecular physics as well, where formally similar systems have been extensively studied [20–23]) yield systems which fulfill all the severe requirements for studying tunneling in the presence of classical Hamiltonian chaos: accurate manipulation of internal and external degrees of freedom, precise control of dissipation and decoherence, and the preparation/detection setup. For a brief account intended for a large audience, see Refs. [24–26]. The aim of the present paper is to suggest challenging experiments that remain to be

*Electronic address: mouchet@celfi.phys.univ-tours.fr
†URL: http://www.phys.univ-tours.fr/~mouchet
‡Electronic address: delande@spectro.jussieu.fr

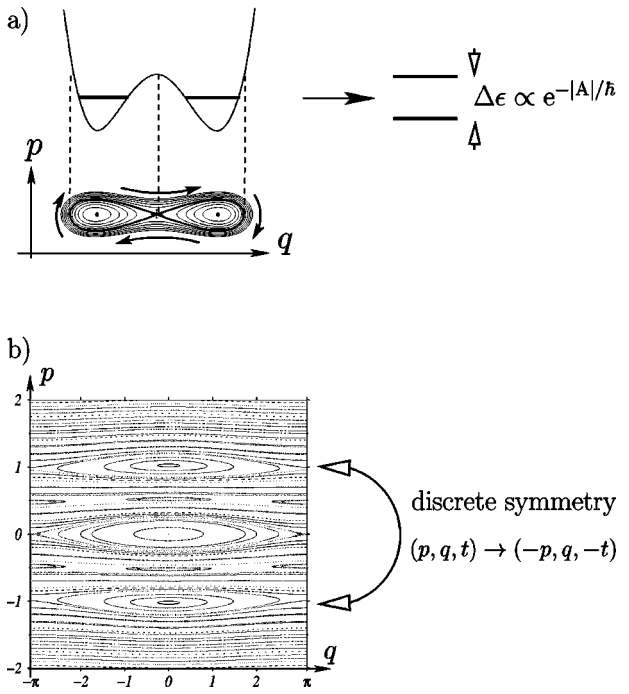

FIG. 1. A generalization of the paradigmatic double-well potential (a) is to consider tunneling between stable islands that are related by any discrete symmetry in phase space; (b) corresponds to Hamiltonian (2) with $\theta=1$ and $\gamma=0.018$. Here, the time reversal symmetry plays the role of parity in (a).

done for reasons which will hopefully become clear in the following.

This paper is organized as follows. In Sec. II we give a general and informal overview. In Sec. III, we briefly recall the main theoretical apparatus that is needed. We implicitly refer to Ref. [14] for details and demonstrations. In Sec. IV, we comment on the results of Refs. [15] and [16]. In Sec. V, we show in this context, with the help of numerical experiments, the very precise form taken by the phenomenon known as chaos-assisted tunneling. We explain why it has not been observed yet with real atoms and propose how to actually bring it to the fore. Before the concluding remarks in Sec. VII, we give in Sec. VI some more numerical results that illustrate how subtle the signatures of chaotic tunneling can be.

II. CHAOTIC TUNNELING

The simplest situation with which to illustrate tunneling is probably the case of a particle in a 1D time-independent symmetric double-well potential [see Fig. 1(a)]. Starting in one well, with an energy that is below the maximum of the potential, a quantum particle can jump into the other well with a nonzero probability, though it is a forbidden classical process. In addition to the classical time scale τ given by the oscillating period *inside* one well, we therefore have a longer time scale: the tunneling period $T \gg \tau$ of the oscillations *between* the wells. In the eigenenergy spectrum, tunneling appears as a quasidegeneracy of the odd- and even-symmetry states whose energies are both of the order of $\hbar/\tau$ but differ by an exponential energy splitting

$$\Delta\epsilon = \frac{2\pi\hbar}{T} \sim e^{-A/\hbar} \tag{1}$$

where A is an $\hbar$-independent typical action and can be interpreted in terms of a unique complex classical trajectory under the barrier [1,27].

In the following we generalize this elementary situation in two ways. First, unlike the parity in the previous example, we can deal with a symmetry which is not necessarily either a spatial one or a twofold one. In other words, we can have any discrete symmetry group acting on the whole phase space as well as any N-fold symmetry which leads to bunches of N-uplets in the energy spectrum (or bands if $N \gg 1$). In the following we keep $N=2$ since we have a twofold symmetry $\mathcal{T}$ actually playing the role of parity [see Fig. 1(b)] and being somehow decoupled from the other discrete symmetries. The classical structure in phase space is globally invariant under $\mathcal{T}$ and the quantum eigenstates can be classified according to their symmetric or antisymmetric character under the unitary transformation which represents $\mathcal{T}$ in the Hilbert space of states. Because $\mathcal{T}$ acts in phase space, it is usually more complicated than a pure spatial transformation. Thus, the two regions of phase space connected by *quantum* tunneling, but *classically* not connected, are in general not separated by a simple potential barrier, but by a more complicated dynamical barrier. In such a case, tunneling is called ''dynamical tunneling'' as suggested by Davis and Heller in Ref. [28]. It often happens that the classically unconnected region are associated with the same region of configuration space, with different momenta. A simple study of the density probability in configuration space is then insufficient to characterize dynamical tunneling; an analysis of the density probablility in momentum space is required.

The second kind of generalization leads to much more puzzling questions. When dealing with systems with several degrees of freedom or, equivalently, if an external time dependence exists, classical trajectories generally lose their regular behavior. They cannot analytically be computed and are organized in a fractal hierarchy that is described by the Kolmosorov-Arnold-Moser (KAM) perturbative scenario. Recently, important progress has been achieved in the understanding of the continuation of these intricate structures in complex phase space and their role at the quantum level (see Refs. [29,30] and especially Ref. [31]). We are therefore led to the following typical quantum chaos question: if one is able to create two symmetric stable islands separated in classical phase space by a chaotic sea whose volume is under control (see Fig. 2), what is the effect of this sea on the (dynamical) tunneling between the islands?

The ''dual'' situation where chaos is created *inside* the wells while the dynamical barrier is kept regular has been introduced and studied theoretically and numerically in Ref. [11]. For a better understanding of what occurs in the energy spectrum when regular wells are separated by a chaotic sea, it was proposed in Ref. [32] to slightly break the tunneling symmetry. Nevertheless, in the present paper, it must be kept in mind that a discrete symmetry will always be maintained

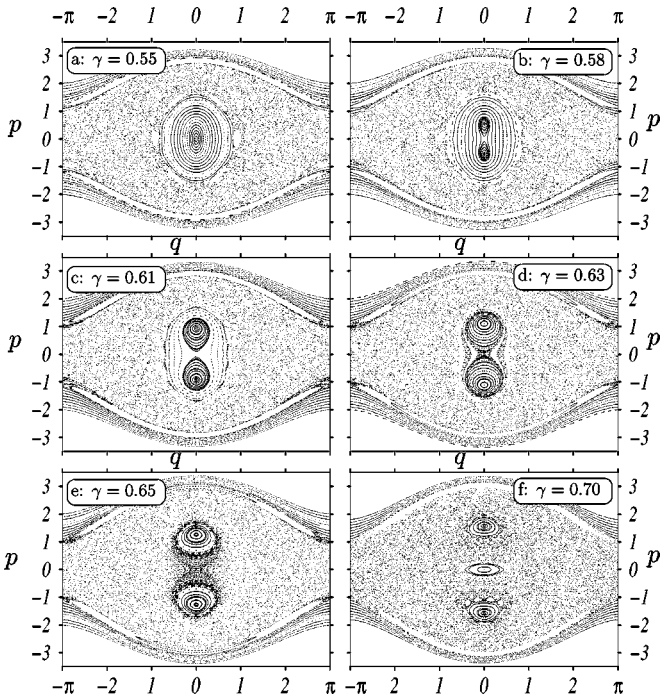

FIG. 2. Poincaré surfaces of section correspond to Hamiltonian 2 at $t=0$ with $\theta=1.724\,137$. Two stable islands in the vicinity of the origin are created by a pitchfork bifurcation at $\gamma\simeq 0.56$. Above this value, chaotic motion progressively invades phase space in between the two stable islands. At $\gamma>\gamma_c\simeq 0.625$, the latter are no longer connected by regular trajectories. The experimental configuration used in the NIST experiments corresponds to $\gamma=0.96$ just before the islands disappear in a bifurcation cascade at $\gamma\simeq 0.97$.

exactly. Finally, a third kind of generalization, where the Hamiltonian character is destroyed by introducing dissipation and/or coupling into a thermal bath, is beyond the scope of this work [33].

III. EFFECTIVE HAMILTONIAN SYSTEM

Following Refs. [14–16] (see also Ref. [34] in a different context) we deal with an effective 1D time-dependent system whose Hamiltonian is

$$H(p,q;t)=\frac{p^2}{2}-\gamma(\theta+\cos t)\cos q \tag{2}$$

in dimensionless units. γ and θ are two classical real parameters that can be modified in real experiments. In addition, there is also one parameter, namely $\hbar_{\rm eff}$, which fixes the quantum scale and is defined by the usual relation between canonical operators: $[q,p]=i\hbar_{\rm eff}$. It turns out that $\hbar_{\rm eff}$ is not constant any longer (see Sec. IV below). It can be also experimentally varied via the rescaling factor that is needed in the canonical commutation relation in order to work in dimensionless units used to write Eq. 2.

The time dependence breaks the conservation of energy, and therefore may generate chaos. In order to deal with such a Hamiltonian, it is crucial to remark that it has both a spatial and a temporal periodicity. The latter implies that the Floquet theorem can be used, which states that the Hilbert space is spanned by an orthonormal eigenbasis of the evolution operator over one period. The corresponding eigenvalues of this unitary operator are distributed on the unit circle and are, therefore, labeled by their phase. This is conveniently written as $\exp(-i2\pi\epsilon/\hbar_{\rm eff})$, where 2π stands for the period of the modulation and ϵ can be interpreted as a quasienergy, a generalization of the notion of energy level for a time-periodic system.

The spatial periodicity of the Hamiltonian is also extremely important, as it makes it possible to split the Hilbert space into independant components, each component being characterized by the so-called Bloch vector k in the $]-0.5,0.5]$ range: under translation of 2π along q, the quasienergy eigenstates are just multiplied by the phase factor $\exp(i2\pi k)$. Thus one has to solve the Floquet-Schrödinger equation in an elementary spatial cell with boundary conditions depending on k. In this way, one generates—for a fixed value of k—a discrete quasienergy spectrum $\epsilon_i(k)$. When the full range of k values is considered, one obtains the familiar (quasi)energy bands [35].

There is an additional discrete symmetry which can be used. The Hamiltonian (2) is invariant under the time-reversal symmetry $(q,p,t)\rightarrow(q,-p,-t)$. In the classical surfaces of section, this implies a symmetry with respect to the q axis. In situations like the one in Fig. 1(b), this implies the existence of pairs of symmetric classically unconnected tori, i.e., a situation where tunneling could be observed. In the quantum world, the situation is slightly more complicated, because this symmetry connects the k subspace to the $-k$ subspace. In the particular case $k=0$ ($k=0.5$ could also be used), this implies that the Floquet eigenstates can be split into two subclasses of states which are either even or odd under the symmetry operation. The splitting between a doublet of even and odd states, $\Delta\epsilon_n=|\epsilon_n^+(0)-\epsilon_n^-(0)|$, will be a measure of tunneling.

We will extensively use the Husimi representation of a quantum state [36]. Such a representation associates with each quantum state $|\psi\rangle$ a phase space function $\psi^{\rm H}(p,q)$ (where p and q are real numbers) defined by

$$\psi^{\rm H}(p,q)=|\langle z|\psi\rangle|^2, \tag{3}$$

where $|z\rangle$ is the coherent state corresponding to the complex number $z=(q+ip)/\sqrt{2\hbar_{\rm eff}}$. Since $|z\rangle$ is a minimal Gaussian wave packet with average momentum p and average position q, the Husimi function $\psi^{\rm H}(p,q)$ contains some information about the degree of localization of $|\psi\rangle$ in phase space. It is then possible to associate quantum states with classical phase space structures.

IV. EXPERIMENTS WITH COLD ATOMS

Under some severe conditions which constrain the experiments, Hamiltonian (2) can be obtained as an effective dimensionless Hamiltonian for cold neutral independent atoms of mass M interacting with two counterpropagating laser beams [14–16]. These two beams have two slightly different frequencies at $\omega_L+\delta\omega/2$ and $\omega_L-\delta\omega/2$. The longitudinal

coordinate x and the dimensionless q are related by $q=2k_L x$, where $k_L=\omega_L/c$. The rescaling of the momentum is given by $p=(2k_L/M\delta\omega)p_x$. γ and θ are fixed by the intensity of the lasers and the detuning of the laser frequencies with respect to the atomic resonance. The dimensionless time t is taken in $\delta\omega^{-1}$ units and the expression of the effective Planck constant is $\hbar_{\rm eff}=8\omega_R/\delta\omega$, where $\omega_R=\hbar k_L^2/2M$. Since *in fine* we want to measure exponentially small tunneling splittings $\Delta\epsilon$, it is necessary to maintain these conditions for a time at least longer than $\hbar_{\rm eff}/\Delta\epsilon$. Moreover, a very accurate control of the preparation of the initial state and of the analysis of the final state is compulsory.

As shown above, due to the temporal and spatial periodicity of the Hamiltonian, observing the standard signature of tunneling—that is, an oscillation of a quantum state between two classically unconnected regions of phase space—requires that a single doublet of Floquet-Bloch eigenstates be initially populated, with well-defined values of the parameters $(\gamma,\theta,\hbar_{\rm eff})$, and a well-defined value of the Bloch angle k. If more than a single doublet is populated, additional frequencies (related to energy differences between the various populated Floquet states) will appear in the temporal evolution. If any parameter is not fixed, the experimental signal will be the superposition of tunneling oscillations (with different frequencies) for various sets of parameters. This will at best—if the dispersion of the parameter values is reasonably small—blur the oscillations at long times and at worst will completely destroy the signature of dynamical tunneling. It is experimentally rather simple to keep an accurate time periodicity of the driving signal, i.e., to fix $\hbar_{\rm eff}$. Similarly, the balance between the constant and the oscillatory term, hence the parameter θ in Eq. (2), is easily controlled. The γ parameter is proportional to the laser intensity and may thus slightly vary across the atomic cloud (because of the transverse structure of the laser beams). The most difficult part is to be sure that a single Bloch angle k is excited. Indeed, this requires a phase coherence of the initial wave function over a large number of laser wavelengths, which is extremely difficult to achieve experimentally [37], as will be shown in the following. In any case, the inhomogeneous broadening of the experimental signal because of the dispersion in k will be responsible for a decay of the tunneling oscillations.

A. NIST experiments [15]

In the NIST experiments, the two stable symmetric islands are chosen quite close in phase space in order to deal with not too small splittings. Another crucial point of this experiment is that the classical motion of the islands over one period, unlike those in Refs. [14] and [16], always remains trapped in one spatial elementary cell of length 2π. The quantum states localized in these islands are consequently only weakly sensitive to the boundary conditions which are governed by the Bloch angle. In other words, the tunneling period will be only weakly dependent on the Bloch angle k. This implies that the unavoidable broadening over k will not spoil too much the signature of tunneling. This is a major improvement over the tunneling described in Refs. [14,16], where a very narrow band of Bloch angle is required to observe clear tunneling oscillations. Moreover, the atoms involved in the tunneling process stay longer in the region where the laser intensities are uniform.

Indeed, as proposed in Ref. [38] and Chaps. 4 and 5 of Ref. [17], the two stable symmetric islands are created from a pitchfork bifurcation of the fixed point at $(p,q)=(0,0)$. To visualize it [see Figs. 2(a) and 2(b)], we extract a one-parameter sequence by varying γ while θ is fixed to the experimentally chosen value in Ref. [15], i.e., $\theta=1.724\,137$. When γ is increased, the pairs of symmetric tori appear at $\gamma\simeq 0.56$. At the center of each set of tori, there is a periodic orbit. Over one period of the driving, the periodic orbit is essentially a rotation over the fixed point at $(p,q)=(0,0)$. This explains that the whole structure remains trapped in a single spatial cell. For $0.56\lesssim\gamma\leqslant\gamma_c$, the tori remain nested in one connected stable island. At $\gamma=\gamma_c\simeq 0.625$, a chaotic sea separates the symmetric islands which shrink and move away from the central point before being dissolved through a cascade of bifurcations starting at $\gamma\simeq 0.97$.

In one series of experiments, $\gamma\simeq 0.96$ and $\hbar_{\rm eff}\simeq 0.8$, the atoms are prepared in one island and their average momentum $\langle p\rangle$ is measured stroboscopically at every modulation period ($=2\pi$ in dimensionless units). Since in phase space the islands rotate about the origin with the same period, no variation in $\langle p\rangle$ would be noticeable if no tunneling occurred. In fact, starting the measurement sequence when $\langle p\rangle$ has its maximum value, oscillations are observed which illustrate the back and forth motion of the atoms between the islands due to dynamical tunneling. The tunneling period T is about 10 modulation periods in this case ($200\ \mu$s). This is in perfect agreement with the quasienergy splitting obtained numerically for the two Floquet eigenstates having the largest Husimi functions inside the islands.

It is worth noting that the NIST group uses a Bose-Einstein condensate as a preliminary step for preparing atoms in well-defined quantum states, especially for achieving a large coherence length for the wave function, i.e., a small spreading of the Bloch angle k. In order to prepare phase space localized states, an optical lattice is carefully turned on. When the tunneling experiment starts, the atomic density and the interaction between atoms is sufficiently small, and the experiment can be described by the interaction of individual independent atoms with the laser beams, i.e., using Hamiltonian (2). However, the cloud of atoms remains cold enough, at a subrecoil temperature, to prevent a large thermal broadening of momentum distribution that would destroy the signal. Because they start from very low temperature, these preparation techniques based on condensate manipulation seem to allow greater room to maneuver than those working with thermal clouds only. Adiabatic switching of the light potentials is not required and one can actually work with values of the classical parameters γ and θ which are far from the perturbative regime of an integrable system.

By diagonalizing the evolution operator corresponding to Eq. (2) over one period, we are not only able to reproduce the oscillatory behavior of $\langle p(t)\rangle$ [see Fig. 3(a)], but also can

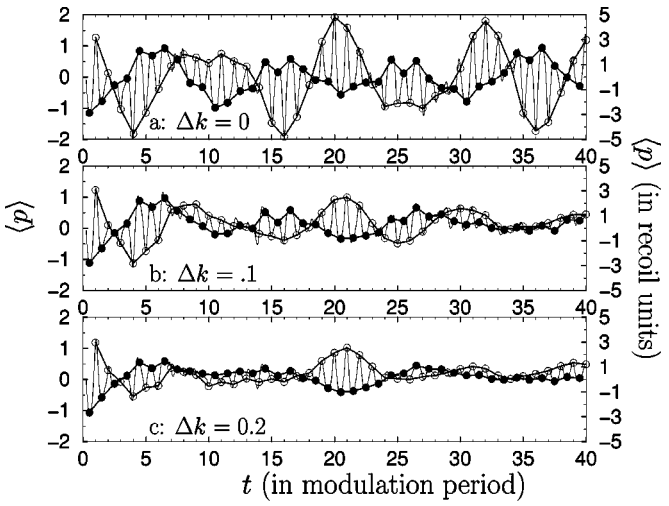

FIG. 3. Numerical simulation of the quantum evolution, in the conditions of the NIST experiment, i.e., $\theta=1.72$, $\gamma=0.96$ and, $\hbar_{\text{eff}}=0.8$ (compare to Fig. 4(a) of Ref. [15]). Starting at $t=\pi/2$ with a Gaussian wave packet whose Husimi function is localized in one stable island (with a vanishing average momentum), we follow the average momentum $\langle p \rangle$ as time evolves. The stroboscopic measurements at times $2\pi+2m\pi$ ($\pi+2m\pi$) with $m\in\{0,1,\ldots,40\}$ are plotted with the white (black) circles. The tunneling oscillations are clearly visible; the tunneling period can be extracted from the typical time scale of the envelope: it is about 10 modulation periods. In the upper plot (a), we assume that a single Bloch angle $k=0$ is initially prepared (which implies a perfect phase coherence of the wave function across the optical lattice). The (thermal) dispersion of the Bloch angle washes out the signal: in case (b), we take a momentum distribution with width $\Delta p=\alpha=2\Delta k=0.2$ and in case (c) $\Delta p=0.4$. In the latter case, the amplitudes of the envelopes are so weak that this corresponds to an upper bound in temperature (about 1/5 of the recoil temperature) at which tunneling can be measured.

study the spoiling effect of the thermal dispersion $\Delta p \propto \sqrt{\text{temperature}}$ and predict the maximum allowed temperature [see Figs. 3(b) and 3(c)] [48]. If α denotes the width of the momentum distribution in recoil momentum units, it can be shown ([14], Sec. 6 A) that it corresponds to a statistical mixture of Bloch states with $\Delta k=\alpha/2$. Figure 3](a) corresponds to the ideal situation where all atoms are prepared with $\alpha \ll 1$ about the $k=0$. When a small but nonvanishing α is introduced, some states of the quasienergy bands with nonvanishing k get involved and blur the tunneling oscillations. For $\alpha=0.2$, the oscillation amplitude is reduced by a factor of 2 and for $\alpha=0.4$ the oscillations nearly disappear. Therefore, in this experiment, having a subrecoil atom cloud is essential.

In the following we want to focus on tunneling only and we will implicitly keep $k=0$.

B. Austin experiments [16]

For a better understanding of the dynamics, one must go beyond the two-level model involving the symmetric and the antisymmetric states only. Other states must be taken into account and their influence can be felt when a classical parameter (γ or θ) or the quantum one ($\hbar_{\text{eff}}$) is continuously varied. Two (quasi)energies may exactly become degenerate if they belong to distinct symmetry classes. If not, they may follow a so-called avoided crossing whose size reflects both the direct coupling between the two states (more precisely, the off-diagonal matrix element of the coupling perturbation) and the indirect coupling to other states. One of the keys to the chaotic tunneling problems is to clearly identify the qualitative nature and the quantitative influence of indirect coupling. This is the background of the Austin experiments.

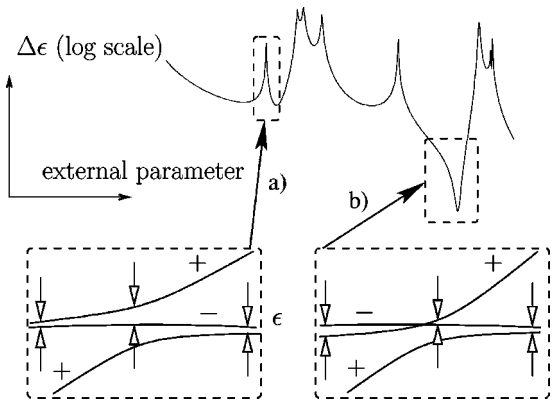

FIG. 4. When a third level is crossing a tunneling doublet when a parameter of the Hamiltonian is varied, there is an avoided crossing between the third level and the member of the doublet with the same symmetry, while the other member of the doublet (with opposite symmetry) ignores the third level. Two generic scenarii exist: in case (a), the tunneling splitting increases in the vicinity of the avoided crossing; in case (b), it decreases and vanishes at a specific value of the parameter.

A third level is involved in a non-negligible indirect coupling when its quasienergy approaches the tunneling doublet energies. This can be understood from perturbation theory, since the leading term of the indirect coupling is proportional to the inverse of the energy difference. The two generic scenarios of the crossing of the doublet by a third state are shown in Fig. 4. Aside from the unavoidable ambiguous definition of the splitting, it appears clear that case (a) corresponds to an increase of the tunneling splitting during the crossing while, conversely, case (b) can lead to arbitrarily small splittings, since an exact degeneracy occurs. Thus, such a crossing by a third state produces a sharp variation of the tunneling period that can be measured experimentally. This is actually what is observed in the Austin experiments and can be confirmed by numerical experiments as shown in Fig. 5. When looking at the Husimi representation of the states, Fig. 6, one can immediately distinguish between the tunneling doublet and the third state sufficiently far from the crossing. As expected, the tunneling doublet has Husimi representations localized in the stable islands, though they also spread in the chaotic sea. On a classical Poincaré surface of section, it is easy to make the difference between chaotic and regular motion; how to transpose this distinction at the quantum level is not known with the large values of $\hbar_{\text{eff}}$ used in both the Austin and the NIST experiments. Some classical structures much smaller than the de Broglie wavelength are possibly present in some of the states [49], but just looking at

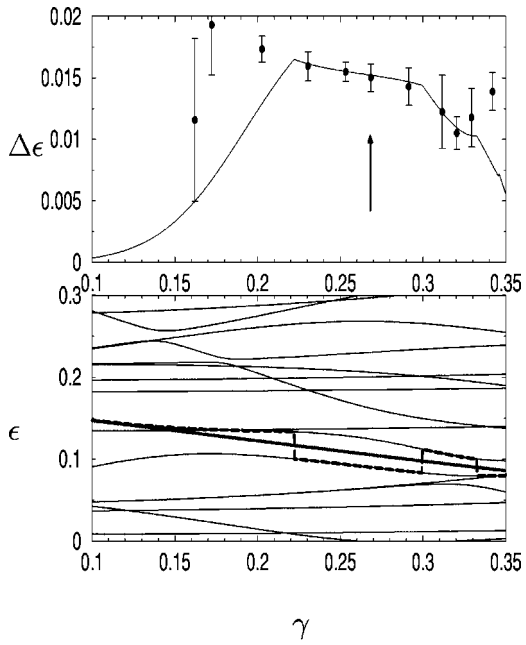

FIG. 5. Numerical results obtained with the parameters of the Austin experiment, that is Hamiltonian (2), with $\theta=1$ and $\hbar_{\rm eff}=0.33$. The lower plot shows a part of the quasienergy spectrum when γ is varied. Thick lines show the two quasienergies whose difference is the tunneling splitting plotted in the upper plot. The two states are selected to have the largest localization of the Husimi function at the center of the stable islands. When a third level couples to the state that belongs to the same symmetry class, an avoided crossing can be seen and the definition of the doublet becomes necessarily ambiguous. There, some discontinuity in the selected state (and in the slope of the tunneling frequency) cannot be avoided. The tunneling splitting is shown as a function of γ in the upper plot, and is compared with the experimental results from Ref. [16]. The agreement is very good, which validates the numerical approach. Around $\gamma=0.2$, a discrepancy is visible. This is precisely the ''ambiguous'' region where the dynamics cannot be reduced to a simple tunneling oscillation, but at least three levels must be taken into account, leading to several relevant energy splittings.

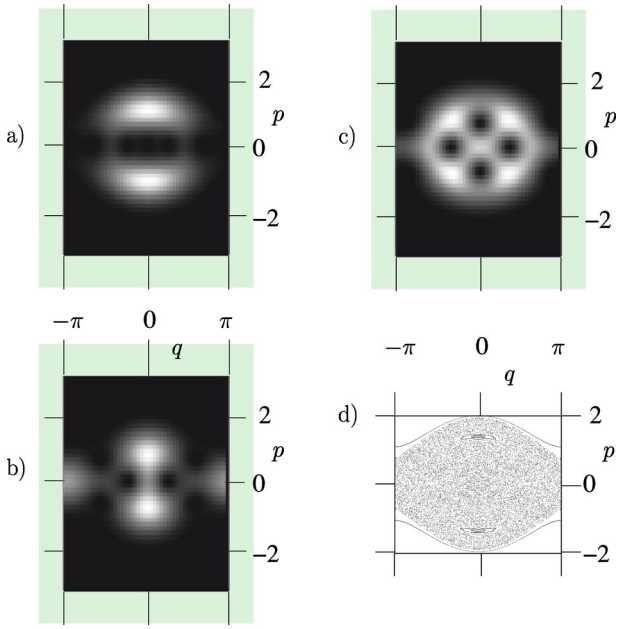

FIG. 6. (a), (b), and (c) show the density in gray scale of the Husimi functions associated with the three states which play an important role for tunneling at $\gamma=0.25$ (parameters of the Austin experiment, as in Fig. 5). As expected, the two members of the doublet, (a) and (b), have their Husimi function localized about the two symmetric islands visible in the classical Poincaré surface of section (d). (b) is strongly coupled to a third states shown in (c). $\hbar_{\rm eff}$ is too large to attribute any regular or chaotic character to the third state. (c) clearly plays a role in the enhancement of the tunneling splitting through an indirect coupling; this is thus an ''assisted tunneling'' mechanism, which cannot be unambiguously characterized as chaos assisted.

the Husimi representation of the third state for $\hbar_{\rm eff}\simeq 1$ does not make it possible to attribute any chaotic or regular character to it. It is only for much smaller $\hbar_{\rm eff}$ that chaotic or regular wave functions make sense. This is not surprising: the dichotomy between regular and irregular motion is a classical one and, at present, it can be extrapolated at the quantum level within the semiclassical regime only. Anyway, one must keep in mind that tunneling only makes sense in the semiclassical regime. One of the great merits of the Austin experiments is that they show a quantum tunneling effect where an indirect process is involved. However, it is an exageration to attribute any chaotic origin to it.

V. NUMERICAL EVIDENCE OF A CHAOTIC TUNNELING REGIME

It was one of the first successes of quantum chaos to have shown that the energy levels of an integrable system are independent of each other, because they are localized on different classical tori, while in chaotic systems level repulsion is the rule. Following the discussion in the preceding section, one may therefore expect that the average size of avoided crossings is increased when chaos is present. The fluctuations of a tunneling process which should be narrow and sparse in an integrable regime should be broader, more numerous, and possibly involving many states in a chaotic regime. We now illustrate this statement in the framework of the experimental atomic Hamiltonian (2).

There are two different ways of rendering chaos observable by quantum eyes: the first one consists of increasing the volume of the chaotic sea with the help of a classical parameter, the second one fixes the classical dynamics and decreases $\hbar_{\rm eff}$. We will present in both ways.

One may try to study the tunneling *fluctuations* separately from the *average behavior*. This average—in a somewhat vague sense—is increased, because chaos diminishes the classical dynamical barrier [50], and this is the reason why the phenomenon can be called chaos assisted tunneling. However, as far as only fluctuations are concerned (there can be an enhancement or a decrease as well), the words ''chaos assisted tunneling'' (CAT) [10] may lead to confusion and we simply use ''chaotic tunneling.'' At last, Brodier, Schlagheck, and Ullmo discovered what they called ''resonant assisted tunneling'' (RAT) [42] to describe an enhancement of tunneling due to an indirect process. It involves one or several quasimodes localized in the secondary resonances surround-

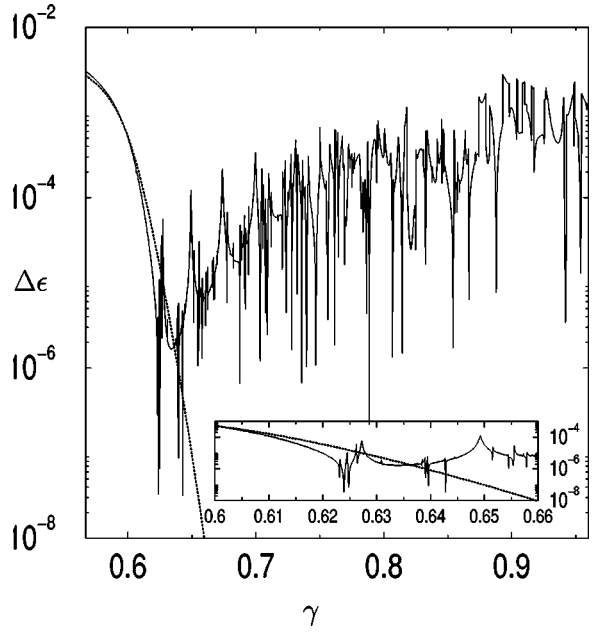

FIG. 7. The tunneling splitting as a function of γ, for $\theta = 1.724\,137$ and $\hbar_{\rm eff} = 0.079\,638$, that is ten times smaller than in the NIST experiments. Two regimes are clearly separated by the critical value $\gamma_c \simeq 0.625$; these two *quantum* regimes correspond to two different *classical* regimes in the Poincaré surfaces of section in Fig. 2. The smooth average decrease with sparse and narrow fluctuations ($\gamma < \gamma_c$) corresponds to the case where the symmetric classical tori belong to the same regular island. The Hamiltonian there can be approximated by a simple integrable Hamiltonian, using the normal form described in the Appendix. The dotted line corresponds to the splitting calculated with this normal form and is in good agreement with the numerical result. In the second regime ($\gamma > \gamma_c$), there are huge quantum fluctuations of the tunneling splitting (and a slightly increased average value). Classically, this corresponds to tunneling between unconnected symmetric islands, separated by a chaotic sea.

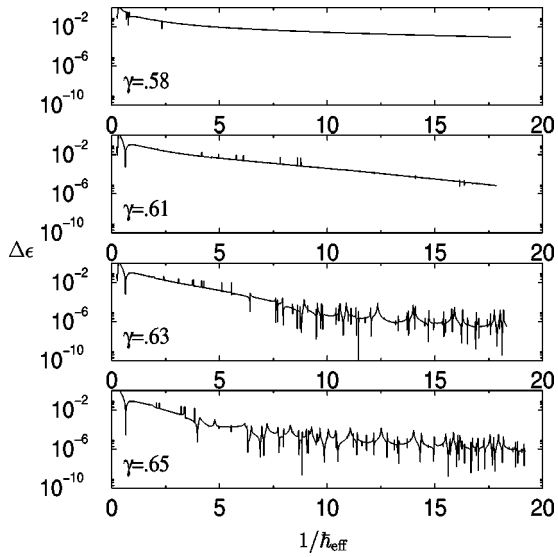

FIG. 8. The tunneling splitting as a function of $\hbar_{\rm eff}$ for fixed values of the classical parameters, i.e., fixed classical dynamics ($\theta = 1.724\,137$ and four values of γ). In the regular regime, an exponential decrease, as described by Eq. (1) is visible as a straight line with a negative slope in a logarithmic scale. The regime of fluctuations can be seen for $\gamma > \gamma_c$ when $\hbar_{\rm eff}$ is small enough for the de Broglie wavelength to be comparable to the size of the chaotic sea between the two islands.

ing the main symmetric islands. Up to now, RAT has been studied quantitatively in a purely quasi-integrable case but there are clues that it can be extended far beyond KAM theory.

A. γ change

Let us first take $\hbar_{\rm eff}$ ten times smaller than the values in the NIST and Austin experiments. It is much easier to do it numerically than experimentally, as it requires the increase of the modulation frequency of the laser beams by one order of magnitude. We then follow the quantum states through the classical bifurcation shown in Fig. 2 and discussed in Sec. IV A. Again, in order to calculate the tunneling splitting $\Delta\epsilon$, we select the states that have the largest Husimi functions inside the islands.

Figure 7 shows that, after a smooth decrease of $\Delta\epsilon$ up to $\gamma = \gamma_c \simeq 0.625$ there is an abrupt change of regime. First, the mean value of $\Delta\epsilon$ increases and second, many fluctuations appear which modify the splitting by several orders of magnitude. It is remarkable that this change of regime can be matched on the Poincaré surfaces of section. The smooth tunneling regime occurs when the resonant tori belong to one quasi-integrable island. For $\gamma < \gamma_c$, we are able to reproduce the main features of tunneling by using an integrable approximation (see Appendix). The decrease of tunneling can be explained in terms of the lengthening of the dynamical barrier. γ_c exactly corresponds to the point where the islands get disconnected. In addition, one can follow the bifurcation on the Husimi representations of the tunneling doublet.

One can hardly detect by eye any regularity in the chaotic regime, but four large spikes in the range $\gamma_c < \gamma < 0.7$ can be seen. This can be traced back to the crossing by the same third state whose quasienergy line is folded four times in the Floquet zone centered on the doublet.

B. $\hbar_{\rm eff}$ change

Figure 8 shows $\Delta\epsilon$ as a function of $1/\hbar_{\rm eff}$ for four values of γ. Here again, two types of regimes, a quasiregular and a chaotic one, can clearly be distinguished. For the values of γ where some substantial chaos is present in between the islands, by decreasing $\hbar_{\rm eff}$ one gets to the chaotic regime. For $\gamma < \gamma_c$, i.e., in the quasiregular regime, one may enter a chaotic regime but for much lower values of $\hbar_{\rm eff}$, since the chaotic layers between KAM tori are so thin that they are not even resolved in the Poincaré surface of section given in the figures.

In these plots, a purely exponential law given by Eq. (1) would produce a straight line with negative slope. For $\gamma < \gamma_c$ and small values of $\hbar_{\rm eff}$, this is also the prediction for the integrable approximation (see Appendix) of the Hamiltonian. Deviations from a pure exponential decrease are observed at low values of $\hbar_{\rm eff}$. This is not surprising, as the

integrable approximation is a local approximation of the Hamiltonian which must fail when large phase space structures are involved. This is, for example, the case for the NIST experiment at $1/\hbar_{\mathrm{eff}} \simeq 1.3$ where the model is only qualitative and predicts a splitting about ten times smaller than that numerically and experimentally observed. However, that the model correctly predicts the behavior at small $\hbar_{\mathrm{eff}}$ values is a strong indication that it is qualitatively correct.

On the other hand, in the chaotic regime, both the integrable model and the exponential law cannot reproduce the fluctuations in the splitting observed in Fig. 8. Whenever such a fluctuation is due to a crossing by a quasimode (and not to a state delocalized in the surrounding chaotic sea), it might be reproduced by the resonance assisted tunneling techniques.

VI. STATISTICAL SIGNATURE OF CHAOTIC TUNNELING?

In order to reproduce quantitatively the statistics of the tunneling splitting fluctuations in the chaotic regime, Leyvraz and Ullmo [43] have introduced a random matrix model. The Hamiltonian can be split into two uncoupled components associated with the even and odd symmetry subspaces. The corresponding matrices are written as

$$H^{\mathrm{even}} = \begin{pmatrix} \epsilon_0^+ & v_1^+ & v_2^+ & \cdots \\ v_1^+ & & & \\ v_2^+ & & H_\perp^+ & \\ \vdots & & & \end{pmatrix} \tag{4}$$

and

$$H^{\mathrm{odd}} = \begin{pmatrix} \epsilon_0^- & v_1^- & v_2^- & \cdots \\ v_1^- & & & \\ v_2^- & & H_\perp^- & \\ \vdots & & & \end{pmatrix}, \tag{5}$$

where $\epsilon_0^\pm$ represent the energies of the doublet, $H_\perp^\pm$ is the Hamiltonian in the chaotic sea (modeled by a random Gaussian matrix), and v is the indirect coupling.

Neglecting direct tunneling consists in taking $\epsilon_0^+ = \epsilon_0^-$. The central hypothesis is to consider all the v's as independent variables with *the same* Gaussian distribution. This is quite natural in order to treat all the other states on the same footing, as they are assumed to be chaotic states randomly delocalized in the chaotic sea. With these assumptions, the splitting distribution can be calculated and is given by a (truncated) Cauchy distribution, see Ref. [43]. For Hamiltonian (2), in each chaotic case where it has been tested, the Leyvraz-Ullmo prediction is in agreement with the numerical results (see Ref. [14]). More surprisingly, we have found that the Leyvraz-Ullmo law gives correct predictions even when the classical dynamics is quasiintegrable (see Fig. 9 and the corresponding Poincaré surface of section in Fig. 1) and the de Broglie wavelength is much larger than the chaotic layers.

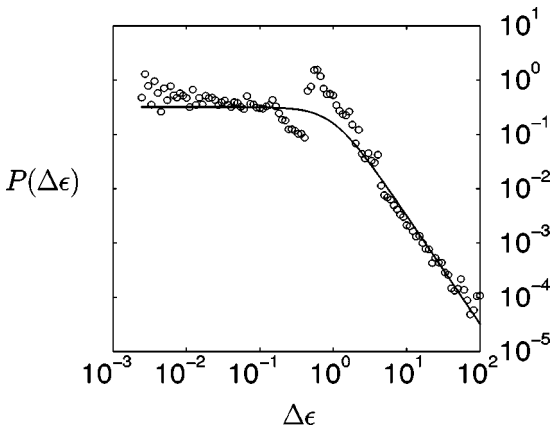

FIG. 9. Statistical distribution of the tunneling splittings as $\hbar_{\mathrm{eff}}$ is varied in the quasiintegrable case corresponding to Fig. 1(b) ($\theta = 1, \gamma = 0.018$). Surprisingly, the numerically observed distribution (small circles) is in good agreement with the Leyvraz-Ullmo law (solid line) which is supposed to be valid in the chaotic case, as it treats all the states coupled to the tunneling doublet on the same footing. This clearly indicates that a Leyvraz-Ullmo distribution is not sufficient to characterize chaotic tunneling.

When looking at the splitting, one observes numerous and large fluctuations (over several orders of magnitude) which were supposed to characterize the chaotic regime. Conversely, we have not been able to find a regular regime of fluctuations with classically chaotic dynamics. Therefore, one must conclude that even though two different regimes of tunneling fluctuations can be identified unambiguously, classical chaos appears to be a sufficient, but not a necessary, condition for having numerous and large fluctuations governed by the Leyvraz-Ullmo law.

These unexpected results are not explained at the present state of the theoretical approaches of chaotic tunneling. If it appears, within future numerical or real experiments, that these results are not due to the peculiar properties of our system, it would definitely mean that further theoretical studies are needed.

VII. CONCLUSION

In this paper we have studied in great detail the transition between a regular and a chaotic regime of tunneling within a classical configuration that can be achieved experimentally. We have shown why $\hbar_{\mathrm{eff}}$ has to be small enough if one wants to reach for the first time the chaotic regime in real systems. In recent experiments with cold atoms, it requires the increase of the modulation period up to one order of magnitude (that is, at least the MHz).

Theoretically, there is also a lot of work to be done if we want to understand and therefore predict the fluctuations quantitatively. The semiclassical regime requires careful study of the dynamics with complex coordinates. However, the present work has shown clearly that the abrupt transition between a regular and a chaotic regime of tunneling corresponds to a classical transition that can be identified very precisely. Tunneling being a relevant concept in a semiclassical regime only, it is therefore not surprising that future

investigations of chaotic tunneling will have to keep track of the classical dynamics in one way or another.

ACKNOWLEDGMENTS

We acknowledge A. Shudo, S. Tomsovic, D. Ullmo, and W. Hensinger for stimulating discussions. A.M. is grateful to N. Mohammedi for his kind reading of the original manuscript and to O. Boebion for computer assistance in the Laboratoire de Mathématiques et de Physique Théorique of Tours and thanks the Laboratoire Kastler Brossel of Paris for kind hospitality. Laboratoire Kastler Brossel de l'Université Pierre et Marie Curie et de l'Ecole Normale Supérieure is Unité Mixtè de Recherche No. 8552 du CNRS. Laboratoire de Mathématiques et de Physique Théorique de l'Université François Rabelais is Unité Mixtè de Recherche No. 6083 du CNRS.

APPENDIX A: INTEGRAL APPROXIMATION NEAR THE PITCHFORK BIFURCATION

When one classical parameter is smoothly varied in a nonintegrable Hamiltonian system, its periodic orbits follow an infinite fractal-like cascade of bifurcations through which they cannot be followed smoothly. However, all the bifurcations can be classified according to a simple set of scenarios: for a given bifurcation of a given periodic orbit, the phase-space dynamics of the original parameter-dependent Hamiltonian can be uniformly approximated by an integrable parameter-dependent Hamiltonian that retains the relevant features only. Of course, because one cannot get rid of the chaotic dynamics, this approximation makes sense only locally, that is, near the periodic orbit, in the neighborhood of the bifurcation. It is the object of the Hamiltonian normal form theory to classify the bifurcations and obtain the simplest form of the approximated integrable Hamiltonians (the so-called normal forms). Generally, i.e., when no constraint or symmetry is present, the one parameter Hamiltonian normal forms have been completely classified by Meyer [30,44,45]. However, the bifurcation shown in Fig. 2 is outside the scope of Meyer's classification precisely because the time reversal symmetry plays a key role. Even if the Poincaré surface of section near the origin [see Fig. 2(b)] cannot be distinguished from that corresponding to Meyer's transitional bifurcation (see, for instance, Fig. 9(b) in Ref. [30]), it is crucial to note that, in our case, two *distinct* 2π-periodic orbits have emerged from the origin. In a transitional bifurcation, the two stable islands would correspond to the *same* 4π-periodic orbit. Therefore, they would be classically connected to each other and would be irrelevant for tunneling. Let us sketch briefly how to obtain the Hamiltonian normal form in our case.

(1) The first step is to find the value γ_0 of γ at which the bifurcation occurs (θ is kept fixed). Such a bifurcation occurs when the trace of the monodromy matrix M_γ at the origin after one period is 2 and corresponds in the $(-2\gamma, 4\gamma\theta)$ plane to the border of the even Arnold tongues (see Fig. 20.1 in Ref. [46]) (the transitional case occurs when $\mathrm{tr}\, M_\gamma = -2$ at the border of the odd Arnold tongues). More precisely, the case shown in Fig. 2 corresponds to $\theta = 1.724\,137$ (the experimental value in the NIST experiment) and the bifurcation takes place at $\gamma_0 \simeq 0.564673$. In the following, we use $\varepsilon = \gamma - \gamma_0$.

Let us denote by $\mathcal{Y}_\varepsilon(z)$ [respectively, $\mathcal{Z}_\varepsilon(z)$] the solution of the Mathieu equation

$$y''(x) + [4\gamma\theta + 4\gamma\cos(2x)]y(x) = 0 \tag{A1}$$

such that $\mathcal{Y}_\varepsilon(0) = 0$ and $\mathcal{Y}'_\varepsilon(0) = 1$ [respectively, $\mathcal{Z}_\varepsilon(0) = 1$ and $\mathcal{Z}'_\varepsilon(0) = 0$]. The prime stands for the derivative with respect to x. For $\varepsilon = 0$, it is straightforward to show that

$$M_{\gamma_0} = \begin{pmatrix} 1 & \dfrac{1}{4\pi}\mathcal{Z}'_0(\pi) \\ 0 & 1 \end{pmatrix}, \tag{A2}$$

where $\mathcal{Z}'_0(\pi) \simeq 1.480\,919$ for $\theta = 1.724\,137$.

(2) The second step is to make a (linear) 2π-periodic canonical change of coordinate that eliminates the time dependence in the quadratic part of Hamiltonian (2), near the origin and uniformly in ε. We are then led to the Hamiltonian

$$\left(-\frac{1}{2}\frac{1}{4\pi}\mathcal{Z}'_0(\pi) + \alpha\varepsilon\right)q^2 + \frac{1}{2}\beta\varepsilon p^2 + \frac{1}{2}\delta\varepsilon p^2 + \text{higher order } 2\pi\text{-periodic terms}, \tag{A3}$$

where α, β, δ are ε-independent coefficients. Only $\beta = 1/\pi\partial_\varepsilon \mathcal{Y}_\varepsilon(\pi)$ evaluated at $\varepsilon = 0$ will be relevant, since α and δ can be eliminated by a suitable canonical change of coordinates following a method explained in Ref. [30], Sec. 4.2. In our case $\beta \simeq 2.008/\pi$. We are therefore led to the following normal form of the quadratic part of the Hamiltonian:

$$\left(-\frac{1}{2}\frac{1}{4\pi}\mathcal{Z}'_0(\pi)\right)q^2 + \frac{1}{2}\beta\varepsilon p^2 + \text{higher order } 2\pi\text{-periodic terms}. \tag{A4}$$

(3) Following the same reasoning that led to the transitional normal form ([30], Sec. 4.2), all higher order 2π-periodic terms except the resonant terms of the form $h_k(\varepsilon)p^k$ can be canceled by a suitable canonical change of coordinates. Because of the time-reversal symmetry, the coefficient h_3 vanishes identically, and therefore the leading order normal form is

$$\left(-\frac{1}{2}\frac{1}{4\pi}\mathcal{Z}'_0(\pi)\right)q^2 + \frac{1}{2}\beta\varepsilon p^2 - \frac{1}{4}h_4(0)p^4. \tag{A5}$$

The explicit calculation of $h_4(0)$ is tedious but it can be estimated numerically by fitting the coordinate $q=0$, $p=\pm\sqrt{\beta\varepsilon/h_4}$ of the satellite 2π-periodic orbits for $\varepsilon>0$. We obtain $h_4\simeq 0.0320$.

It is far from obvious that the quantization of the normal form (A5) will give a good approximation of the quasienergies of the tunneling doublet. Some discrepancies may arise from the fact that quantum physics is invariant under canonical transformations only at the leading order in $\hbar$. When we replace p with q and change the sign of the energies, the normal form (A5) leads to a standard 1D double-well problem whose quantum spectrum can be found by numerically diagonalizing the Hamiltonian written in a harmonic basis. The tunneling splitting of the ground doublet is given by the dotted line in Fig. 7 and it agrees reasonably well with the exact numerical result for γ near γ_0.

[1] A. Messiah, *Mécanique Quantique* (Dunod, Paris, 1964) (English translation published by North-Holland, Amsterdam, 1964).

[2] R. Balian and C. Bloch, Ann. Phys. (N.Y.) **84**, 559 (1974).

[3] M. Wilkinson, Physica D **21**, 341 (1986).

[4] M. Wilkinson and J.H. Hannay, Physica D **27**, 201 (1987).

[5] *Chaos et Physique Quantique—Chaos and Quantum Physics*, Les Houches, École d'Été de Physique Théorique 1989, Session LII, edited by M. Giannoni, A. Voros, and J. Zinn-Justin (North-Holland, Amsterdam, 1991).

[6] C. Dembowski, H.-D. Gräf, A. Heine, R. Hofferbert, H. Rehfeld, and A. Richter, Phys. Rev. Lett. **84**, 867 (2000).

[7] W.A. Lin and L.E. Ballentine, Phys. Rev. Lett. **65**, 2927 (1990).

[8] O. Bohigas, D. Boosé, R. Egydio de Carvalho, and V. Marvulle, Nucl. Phys. A **560**, 197 (1993).

[9] O. Bohigas, S. Tomsovic, and D. Ullmo, Phys. Rep. **223**, 43 (1993).

[10] S. Tomsovic and D. Ullmo, Phys. Rev. E **50**, 145 (1994).

[11] S.C. Creagh and N.D. Whelan, Phys. Rev. Lett. **77**, 4975 (1996).

[12] O. Brodier, P. Schlagheck, and D. Ullmo, Ann. Phys. (N.Y.) **300**, 88 (2002).

[13] J. Zakrzewski, D. Delande, and A. Buchleitner, Phys. Rev. E **57**, 1458 (1998).

[14] A. Mouchet, C. Miniatura, R. Kaiser, B. Grémaud, and D. Delande, Phys. Rev. E **64**, 016221 (2001).

[15] W.K. Hensinger, H. Häffner, A. Browaeys, N.R. Heckenberg, K. Helmerson, C. McKenzie, G.J. Milburn, W.D. Phillips, S.L. Rolston, H. Rubinsztein-Dunlop, and B. Upcroft, Nature (London) **412**, 52 (2001).

[16] D.A. Steck, H.O. Windell, and M.G. Raizen, Science **293**, 274 (2001).

[17] W.K. Hensinger, Ph.D thesis, The University of Queensland, Autralia, 2002.

[18] W.K. Hensinger, A. Mouchet, P.S. Julienne, D. Delande, N.R. Heckenberg, and H. Rubinsztein-Dunlop, Phys. Rev. A (to be published).

[19] *Laser and Manipulation of Atoms and Ions*, Enrico Fermi International Summer School, Course CXVIII, 9–19 July 1991, edited by E. Arimondo, W.D. Phillips, and F. Strumia (North-Holland, Amsterdam, 1992).

[20] R.T. Lawton and M.S. Child, Mol. Phys. **44**, 709 (1981).

[21] E.L. Sibert, W.P. Reinhardt, and J.T. Hynes, J. Chem. Phys. **77**, 3583 (1982).

[22] M.E. Kellman and E.D. Lynch, J. Chem. Phys. **87**, 5386 (1987).

[23] J.P. Rose and M.E. Kellman, J. Chem. Phys. **105**, 7348 (1996).

[24] E.J. Heller, Nature (London) **412**, 33 (2001).

[25] A. Mouchet and D. Ullmo, Phys. World **14**(9), 24 (2001).

[26] B. Goss Levi, Phys. Today **54**(8), 15 (2001).

[27] J. Heading, *An Introduction to Phase-Integral Methods* (Methuen, Wiley, London, 1962).

[28] M.J. Davis and E.J. Heller, J. Phys. Chem. **85**, 307 (1981).

[29] M. Kuś, F. Haake, and D. Delande, Phys. Rev. Lett. **71**, 2167 (1993).

[30] P. Lebœuf and A. Mouchet, Ann. Phys. (N.Y.) **275**, 54 (1999).

[31] A. Shudo and K.S. Ikeda, Physica D **115**, 234 (1998).

[32] S. Tomsovic, J. Phys. A **31**, 9469 (1998).

[33] *Tunneling in Complex Systems*, edited by S. Tomsovic, Proceedings of the Institute for Nuclear Theory Vol. 5 (World Scientific, Singapore, 1998).

[34] V. Averbukh, N. Moiseyev, B. Mirbach, and H.J. Korsh, Z. Phys. D: At., Mol. Clusters **35**, 247 (1995).

[35] N.W. Ashcroft and N.D. Mermin, *Solid State Physics* (Saunders College, Philadelphia, 1976).

[36] K. Husimi, Proc. Phys. Math. Soc. Jpn. **22**, 264 (1940).

[37] M. Greiner, O. Mandel, T. Esslinger, T.W. Hänsch, and I. Bloch, Nature (London) **415**, 39 (2002).

[38] W.K. Hensinger, B. Upcroft, N.R. Heckenberg, G.J. Milburn, and H. Rubinsztein-Dunlop, Phys. Rev. A **64**, 063408 (2001).

[39] R. Luter and L.E. Reichl, Phys. Rev. A **66**, 053615 (2002).

[40] W.H. Zurek, Nature (London) **412**, 712 (2001).

[41] N.L. Balazs and A. Voros, Ann. Phys. (N.Y.) **199**, 123 (1990).

[42] O. Brodier, P. Schlagheck, and D. Ullmo, Phys. Rev. Lett. **87**, 064101 (2001).

[43] F. Leyvraz and D. Ullmo, J. Phys. A **29**, 2529 (1996).

[44] K.R. Meyer, Trans. Am. Math. Soc. **149**, 95 (1970), reprinted in Ref. [47].

[45] K.R. Meyer and G.H. Hall, *Introduction to Hamiltonian Dynamical Systems and the N-Body Problem*, Applied Mathematical Sciences Vol. 90 (Springer-Verlag, New York, 1992).

[46] M. Abramowitz and I.A. Segun, *Handbook of Mathematical Functions* (Dover Publications, New York, 1965).

[47] R.S. Mackay and J.D. Meiss, *Hamiltonian Dynamical Systems* (Adam Hilger, Bristol, 1987).

[48] After the first version of the present paper was written, we learned that an independent numerical work [39] had obtained the same results as those in our Fig. 3(a). But Ref. [39] does not consider the thermal effects and does not always work within the Floquet theory at $k=0$ instead of the Floquet-Bloch theory. In the present work we clearly demonstrate that thermal effects cannot be neglected and must be studied carefully when experiments are discussed.

[49] From time to time, it is claimed [40] that a simple matching between classical structures and quantum wave sub-Planckian

structures was found but, as was understood a long time ago (Ref. [41]), the latter are generally washed out as soon as one tries to measure global averages.

[50] The question of defining an integrable system with which the chaotic one should be compared is extremely difficult because of the exponential sensitivity of tunneling to the classical parameters. It is a much more serious problem than defining an averaging procedure.